Vibrational properties of AlN grown on (111)-oriented silicon

T. Prokofyeva, M. Seon, J. Vanbuskirk, and M. Holtz*
Department of Physics, Texas Tech University, Lubbock, Texas 79409

S. A. Nikishin, N. N. Faleev, and H. Temkin
Department of Electrical Engineering, Texas Tech University, Lubbock, Texas 79409

S. Zollner
Motorola Semiconductor Products Sector, Process and Materials Characterization Laboratory, MD M360, 2200 West Broadway Road, Mesa, Arizona 85202

(Received 15 June 2000; published 7 March 2001)

We study the vibrational spectrum of AlN grown on Si(111). The AlN was deposited using gas-source molecular beam epitaxy. Raman backscattering along the growth c axis and from a cleaved surface perpendicular to the wurtzite c direction allows us to determine the E_2^1, E_2^2, A_1(TO), A_1(LO), and E_1(TO) phonon energies. For a 0.8-μm-thick AlN layer under a biaxial tensile stress of 0.6 GPa, these are 249.0, 653.6, 607.3, 884.5, and 666.5 cm^{-1}, respectively. By combining the Raman and x-ray diffraction studies, the Raman stress factor of AlN is found to be $-6.3\pm1.4\ cm^{-1}$/GPa for the E_2^2 phonon. This factor depends on published values of the elastic constants of AlN, as discussed in the text. The zero-stress E_2^2 energy is determined to be 657.4 $\pm0.2\ cm^{-1}$. Fourier-transform infrared reflectance and absorption techniques allow us to measure the E_1(TO) and A_1(LO) phonon energies. The film thickness (from 0.06 to 1.0 μm) results in great differences in the reflectance spectra, which are well described by a model using damped Lorentzian oscillators taking into account the crystal anisotropy and the film thickness.

DOI: 10.1103/PhysRevB.63.125313 PACS number(s): 78.30.Fs, 78.20.−e, 78.66.Fd, 62.20.Dc

I. INTRODUCTION

The physical properties of hexagonal aluminum nitride have recently become of great interest.[1] It has the largest energy band gap among the III-N compounds of InN, GaN, and AlN. As an alloy family, these compounds permit the growth of semiconductors having energy gaps ranging from 1.9 to 6.2 eV. AlN also has a large thermal conductivity, high thermal stability, and high hardness, is an excellent electrical insulator, and is piezoelectrically active. These properties are both physically interesting and technologically important.[1–3]

Epitaxial growth of nitride semiconductors uses sapphire, SiC, or Si substrates. The film properties of AlN are strongly influenced by the substrate materials.[4] Using silicon as the substrate is highly attractive for device applications due to potential integration with well-developed silicon technologies. The large differences between the lattice constants of AlN and Si make the growth of high-quality material very difficult. Recently, growth of high-quality AlN has been demonstrated on (111)-oriented silicon substrates using molecular beam epitaxy (MBE).[5–12] Despite their importance, many of the physical properties of crystalline AlN have not been fully investigated, specifically when it is epitaxially deposited on a substrate.

In this paper, we examine the vibrational properties of AlN grown on silicon substrates. These studies are carried out using Fourier-transform infrared spectroscopy (FTIR) and Raman scattering. We find only two FTIR reports on bulk-grown AlN (Refs. 13 and 14) and a few articles concerning FTIR studies of crystalline AlN deposited on silicon.[4,15–19] The E_1 and A_1 phonons are infrared active in the wurtzite crystal structure.[20] We find no detailed discussion of the effects of anisotropy on the AlN reflectance spectrum. Four primary effects influence the optical properties of anisotropic semiconductors in the infrared region, as has been recently discussed by Tiwald *et al.*, in connection with silicon carbide.[21] These effects are the optical anisotropy of the wurtzite crystal structure, film thickness, epilayer doping, and substrate conductivity.[22] MacMillan, Devaty, and Choyke discuss the presence of anisotropy in the dielectric function of AlN.[15] However, use of an anisotropic model was not critical in their case due to the small angle of incidence (5°) used in the experiments. Our results for AlN on silicon are well described based on the anisotropy of the dielectric function and thin-film effects.

Raman scattering has been used extensively to study III-nitride semiconductors, including AlN. There are only a few reports concerning the Raman spectrum of crystalline AlN grown on silicon.[4,16–19] Six phonons, E_2^1, E_2^2, A_1(TO), A_1(LO), E_1(TO), and E_1(LO), are allowed in Raman scattering from wurtzite crystals.[20] The E_1(LO) band is only seen in right-angle scattering, e.g., $y(xz)\overline{x}$, using the standard Porto notation. The c axis of the AlN crystal is defined as the z direction, and x and y are perpendicular to z. The wurtzite-structure phonon symmetries, together with allowed configurations for Raman backscattering, are summarized in Table I. In this work, we measure all AlN phonons that are allowed in Raman backscattering.

The primary focus of our work is the determination of the substrate-induced stress in the AlN. The stress is primarily due to differences in the thermal expansion coefficients as the epitaxial layer and substrate cool from the growth temperature to ambient conditions.[23] Stress is important because

TABLE I. AlN (wurtzite) phonon symmetries, allowed backscattering configurations, and measured energies. Phonon energies determined by FTIR spectroscopy are also included.

Phonon symmetry	Raman-allowed backscattering	Raman phonon energy (cm^{-1})[a,b]	Raman phonon energy (cm^{-1})[c]	FTIR phonon energy (cm^{-1})[d]
E_2^1	$z(yx)\bar{z}$, $z(yy)\bar{z}$, $x(yy)\bar{x}$	249.0±0.4	248.6±0.2	
E_2^2	$z(yx)\bar{z}$, $z(yy)\bar{z}$, $x(yy)\bar{x}$	653.6±0.2	657.4±0.2	
A_1(TO)	$x(yy)\bar{x}$, $x(zz)\bar{x}$	607.3±0.2	611.0±0.2	
E_1(TO)	$x(yz)\bar{x}$	666.5±0.2	670.8±0.2	665[e,f]
A_1(LO)	$z(yy)\bar{z}$	884.5±0.2	890.0±0.2	884[e]

[a]This work.
[b]AlN film thickness 0.80 μm. Tensile stress 0.6 GPa.
[c]Relaxed phonon energies from Ref. 35.
[d]AlN film thickness 0.06 μm.
[e]From reflectance.
[f]From absorption.

it alters the energy band structure and can influence the epilayer properties, even resulting in layer cracking.[24,25] Raman scattering is a proven method for studying stress. The E_2^2 Raman band has been used extensively to study the substrate-induced biaxial stress in GaN.[23,26–28] However, for AlN we find no published reports establishing the relationship between known stress and the E_2^2 phonon energy. Published values of the E_2^2 phonon energy in unstressed AlN are varied, ranging from 655 to 665 cm^{-1}.[29–31] Phonon-stress relationships are established best using externally applied, uniaxial stress, such as what has been extensively reported for silicon.[32] An alternative, which is appropriate for epitaxial films, is to examine the effects of biaxial stress on the Raman spectrum. This relationship is extremely important because it allows one to measure the *compressive* or *tensile* stress in AlN layer deposited on *any* of the commonly used substrates.

We combine Raman and x-ray diffraction (XRD) studies to obtain the Raman-stress factor for undoped AlN under tensile biaxial stress. Two quantities are necessary: the phonon energy under no stress and that at some known biaxial stress. Thus, the Raman-stress factor (k) is obtained using

$$\Delta\omega = k\sigma_{\perp}, \tag{1}$$

where $\Delta\omega$ is the shift in the phonon energy due to biaxial stress ($\sigma_{\perp}$) perpendicular to the growth (c) axis. Tensile (compressive) stress corresponds to $\sigma_{\perp} > 0$ (< 0). Typically, strain is measured using XRD; then the corresponding stress is found from the elastic constants. A range of values has been reported for the AlN elastic constants both from experiment[33–36] and theory.[37–39] Knowledge of the elastic constants is essential in determining the stress/strain relationship.

II. EXPERIMENTAL METHODS

AlN layers were grown at 1100–1160 K using gas-source molecular beam epitaxy (GSMBE) with ammonia on (111)-oriented silicon substrates. Details of the growth are described in Refs. 9–11. Epitaxial layers varied from 0.06 to 1.0 μm in thickness. The AlN epilayers were not intentionally doped. Secondary-ion mass spectroscopy measurements show the impurity concentrations of silicon and carbon to be $< 2\times10^{17}\,cm^{-3}$ and oxygen to be $\approx 5\times10^{18}\,cm^{-3}$.[40] For this oxygen concentration, it is possible that there is internal ''hydrostatic'' stress within our samples. However, we have made no systematic studies of the effects of oxygen on the vibrational properties of AlN, similar to what has been done in Ref. 26 for intentional (substitutional) doping of GaN.

All *ex situ* studies reported here were done with the samples at room temperature. The smoothness of the AlN was determined using atomic-force microscopy. Over the $5\,\mu m\times 5\,\mu m$ areas scanned, the rms roughness of our samples ranged from 0.5 to 1.9 nm. This roughness is typical for our AlN/Si epilayers.[9] Smooth surfaces are very important for certain optical studies, such as FTIR and ellipsometry.

XRD studies were done primarily to determine the c-axis lattice parameter. The measurements were carried out using a high-resolution diffractometer with Ge(220), fourfold, Bartels-type monochromator and a Ge(220) threefold analyzer crystal. The illumination region for the XRD measurements is approximately $0.2\,mm\times 6\,mm$. Triple-crystal $2\theta-\omega$ and ω rocking curves (RC) have been measured for the (0002) AlN reflection. A typical diffraction pattern, obtained from a 0.2-μm-thick AlN epilayer, is shown in Fig. 1. The $2\theta-\omega$ measurement of the (0002) reflection permits us to evaluate the lattice parameter c. The full width at half maximum (FWHM) of the (0002) peak in Fig. 1 has a value of 100±5 arcsec. This corresponds to a structural coherence length of 165±8 nm along the growth direction. Our results show that the coherence length closely matches our nominal epilayer thickness, indicating high crystal perfection. We note that the difference between sample thickness and coherence length is plausibly explained by the presence of a region near the AlN-substrate interface that possesses a relatively high defect density.[9,10]

FTIR spectra were measured over the 400–4000-cm^{-1} range with a spectral resolution of 4 cm^{-1}. For the absorp-

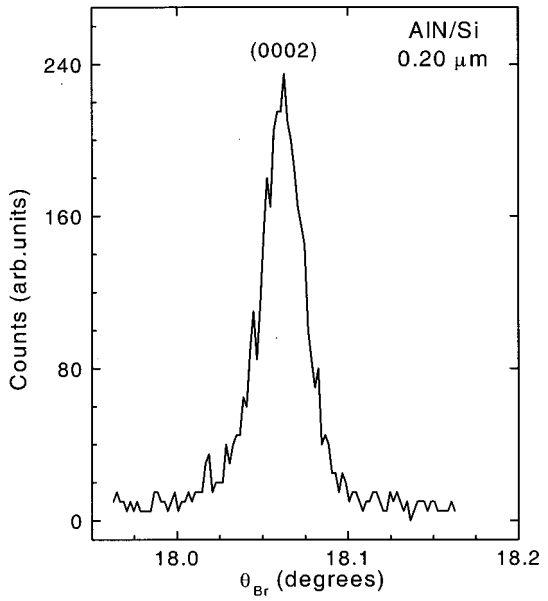

FIG. 1. X-ray diffraction data (2θ–ω) obtained from the (0002) reflection of an AlN/Si(111) layer 0.2 μm in thickness.

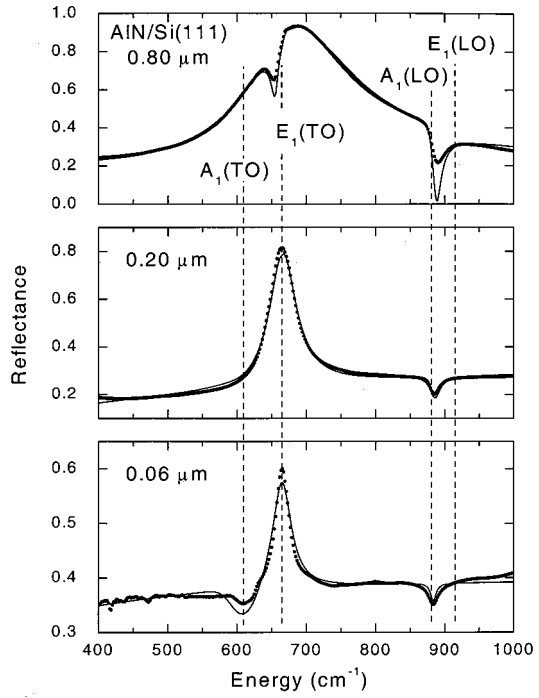

FIG. 2. FTIR reflectance spectra of AlN on Si(111) with different epilayer thicknesses. The symbols are the data sets, and solid curves are calculated using the anisotropic dielectric function and Fresnel relations for thin films backed by a substrate. The phonon energies used to calculate the spectra are indicated by the vertical dashed lines.

tion, a high-resistivity substrate (1000–4000 Ω cm) with the back surface polished, was used to permit transmission of light through the sample. We used unpolarized light with a 30° angle of incidence for the FTIR reflectance studies. These spectra were taken using AlN grown on both high-resistivity silicon (1000–4000 Ω cm, back side polished) and low-resistivity, *n*-type silicon (0.05–0.03 Ω cm, rough back surfaces).

Raman spectra were generated using 488.0-nm light, focused to a spot ≈ 2 μm in diameter, and direct backscattering.[28] Standard optical elements were used for the polarization studies. Scattered light was passed through a holographic notch filter, dispersed by a 0.5-m spectrometer, and detected using a charge-coupled device (CCD) array. This system allows us to measure a spectral range of ≈ 600 cm^{-1} in a single exposure of 2 to 30 min with a 2-cm^{-1} instrument bandpass. Calibration was done using emission lines from a neon lamp or laser plasma lines, giving a wave-number precision of 0.2 cm^{-1} for peak position determination.

III. FTIR REFLECTANCE AND TRANSMITTANCE OF AlN/Si

Figure 2 shows FTIR reflectance spectra taken from samples with thicknesses 0.06, 0.20, and 0.80 μm. The spectral range shown corresponds to the transverse and longitudinal-optical-phonon energy range. For the 0.8-μm thickness, the reflectance shows a broad, asymmetric feature with two minima. This is reminiscent of a reststrahlen band bracketed by transverse- and longitudinal-optical-phonon energies. Because we study a thin film, the reststrahlen band shows a pronounced asymmetry. With thinner AlN films, the spectra in Fig. 2 evolve to show one maximum and one minimum, which are most closely associated with the E_1(TO) and A_1(LO) phonons, respectively. We find that the spectra can be described based on a model in which the thickness of the AlN is the primary parameter varied.

FTIR reflectance spectra were modeled using Lorentz oscillators for the dielectric functions, which take into account the uniaxial anisotropy of the AlN. In the presence of uniaxial anisotropy, the dielectric tensor ε has the diagonal form[41]

$$\varepsilon = \begin{bmatrix} \varepsilon_\perp & & \\ & \varepsilon_\perp & \\ & & \varepsilon_\parallel \end{bmatrix}, \tag{2}$$

where $\varepsilon_\perp(\varepsilon_\parallel)$ is the ordinary (extraordinary) dielectric response to fields perpendicular (parallel) to the wurtzite *c* axis. The dielectric functions are

$$\varepsilon_{\parallel,\perp} = \varepsilon_{\infty\parallel,\perp} + \frac{\varepsilon_{\infty\parallel,\perp}(\omega^2_{\mathrm{LO}\parallel,\perp} - \omega^2_{\mathrm{TO}\parallel,\perp})}{\omega^2_{\mathrm{TO}\parallel,\perp} - \omega^2 - i\omega\Gamma_{\parallel,\perp}}. \tag{3}$$

Here, $\omega_{\mathrm{LO}\parallel}$ and $\omega_{\mathrm{TO}\parallel}$ are the A_1-symmetry LO- and TO-phonon energies, respectively. Likewise, $\omega_{\mathrm{LO}\perp}$ and $\omega_{\mathrm{TO}\perp}$ are the E_1-symmetry LO-and TO-phonon energies. The high-frequency dielectric functions are $\varepsilon_{\infty\parallel} \approx \varepsilon_{\infty\perp} = 4.84$.[13] The damping constants ($\Gamma_\parallel$ and $\Gamma_\perp$) and the phonon energies are parameters in the model. The stress field is not explicit in Eq. (2) because biaxial stress perpendicular to the *c* axis will not lower the crystal symmetry, leaving the form of the dielectric tensor unchanged. Stress enters through the phonon energies in Eq. (3). Reflectance is calculated at the experimental angle

of incidence (30°) using these dielectric functions and the Fresnel relations for thin dielectric films on a substrate.[42] The AlN thickness enters as a parameter in the Fresnel relations. The 0.06-μm sample thickness was determined using spectroscopic ellipsometry. The thicknesses of the other samples shown in Fig. 2 were determined to be 0.20 ± 0.03 and 0.80 ± 0.03 μm from the Fabry-Perot fringes in uv-visible reflectance. Our FTIR reflectance model yielded respective thicknesses of 0.06, 0.16, and 0.80 μm. The energy-dependent optical properties of silicon were used for the reflectance calculation.[41] The substrate thickness was set to that of our wafers (about 0.5 mm). The incoherent interference of front and back surface reflections was taken into account. The reflectance of the back surface was varied to obtain good agreement with the data. This primarily accounts for the smoothness of the back surface.

Results of the model reflectance spectra are shown in Fig. 2, along with the data. The agreement seen between the model and the data in Fig. 2 is good for each thickness. The E_1(TO) phonon energy found from modeling our data lies in the 665–666-cm^{-1} range. The A_1(LO) phonon has energy between 883 and 885 cm^{-1}. We fix the E_1(LO) phonon energy at 912 cm^{-1} (Ref. 35) and that of the A_1(TO) phonon is held at 607 cm^{-1} based on our Raman measurements. The model is not as sensitive to the values used for the E_1(LO) and A_1(TO) phonon energies. These are determined within ±5 cm^{-1} from these studies. Table I shows our phonon energies to be in good agreement with previous studies[13,18,31,34,43] and with our Raman measurements. Variations by several cm^{-1} can be attributed to changes in the epilayer stress, to be discussed in the next section. The broadening parameters ranged from 8 to 19 cm^{-1}. These values are consistent with recent infrared spectroscopic-ellipsometry measurements of AlN grown on sapphire using metal-organic vapor phase epitaxy[43] and are smaller than what is obtained in films deposited on sapphire using plasma-enhanced chemical vapor deposition.[18] We note also a larger reflectance background in the data from the 0.06-μm-thick sample in Fig. 2. This is because the substrate used had its back surface polished for the transmission measurements. We have adjusted the reflection from the polished back surface of the substrate so that we have a good match in the background level. The dip near 620 cm^{-1} is from two-phonon (TA+TO) absorption in the silicon substrate[44] and is not associated with the A_1(TO) phonon of AlN.

An interesting result of the FTIR reflectance measurements is that they are sensitive to the E_1(TO) and A_1(LO) phonons. The former is not surprising, since the E_1(TO) phonon is allowed to interact with infrared radiation at this energy when the light propagates along the *c* axis. However, the high-frequency shape of the reststrahlen band is generally dictated by the LO phonon of the same symmetry. The minimum in reflectance seen from the A_1(LO) phonon is interesting, since the A_1-symmetry vibrations should interact with light that does not propagate strictly along the *c* axis. For *p* polarization, the oscillating electric field has components both parallel and perpendicular to the *c* axis, inducing responses from both $\varepsilon_{\parallel}$ and $\varepsilon_{\perp}$. Because the dielectric functions vary strongly, especially in the energy range between

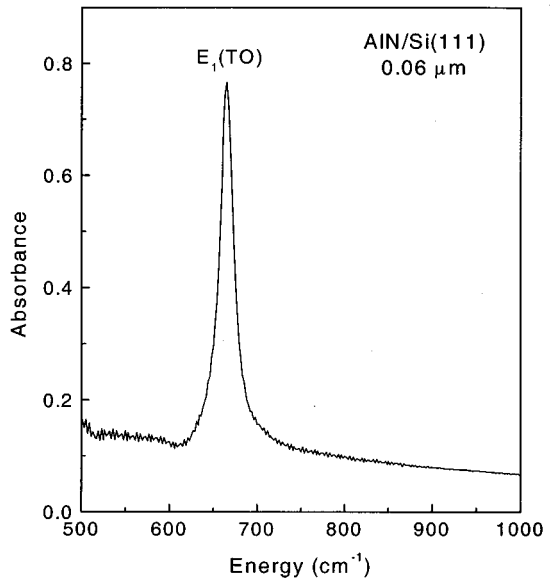

FIG. 3. FTIR absorption spectrum of a 0.06-μm-thick AlN grown on high-resistivity silicon. Only the E_1(TO) phonon interacts with light incident along the *c* axis (sample normal).

the A_1(LO) and E_1(LO) phonons, light refracts away from the *c* axis (normal). This gives rise to interaction with $\varepsilon_{\parallel}$ and results in the allowed A_1 scattering. This situation has been discussed in detail by Tiwald *et al.*, regarding their infrared ellipsometry studies of SiC.[41]

Figure 3 shows the FTIR transmission spectrum of a 0.06-μm-thick sample grown on high-resistivity silicon. For light incident normal to the sample surface, we see only the allowed E_1(TO) absorption band at 665 cm^{-1}. From the FTIR absorption measurement the experimental phonon line width is 17 cm^{-1}. AlN deposited on Si(111) by reactive magnetron sputtering and pulsed laser deposition showed very broad absorption bands that ranged in peak position from 665 to 706 cm^{-1}, depending on the deposition conditions.[17] They attribute the large shifts and linewidths to stress distributions within the AlN. Our much narrower linewidth indicates uniform stress, consistent with the Raman measurements we now discuss.

IV. RAMAN MEASUREMENTS OF AlN/Si AND THE RAMAN-STRESS RELATIONSHIP

Figure 4 shows Raman spectra taken under different scattering and polarization configurations from a 0.8-μm-thick AlN layer. We observe all AlN phonons allowed in backscattering, in agreement with the expected selection rules.[20] The intense band at 520 cm^{-1} is the O(Γ) phonon from the silicon substrate. The features near 620 and 830 cm^{-1} are also from the substrate. Clear from this figure is the low scattering intensity from the 0.8-μm-thick AlN. The intensities from the AlN E_2^2 phonon, which is the strongest band observed, were smaller for thinner epitaxial layers and comparable to that of the substrate bands at 620 and 830 cm^{-1}.

AlN phonon energies are summarized in Table I. Except for the E_2^1 band, all modes red shift relative to their respec-

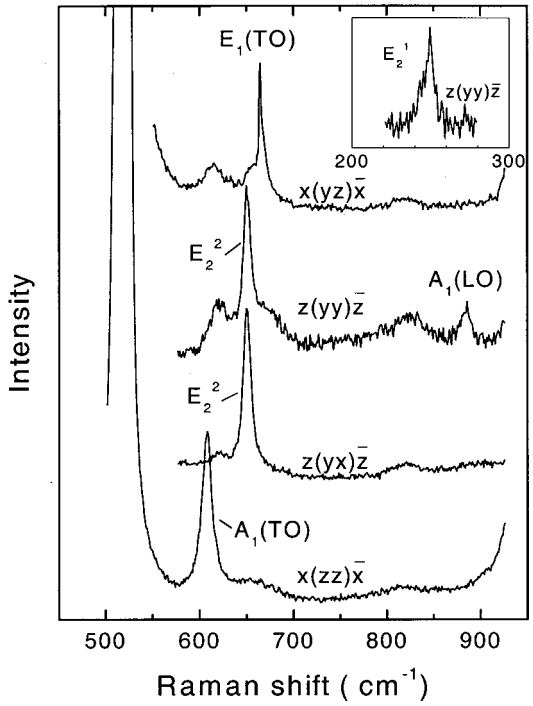

FIG. 4. Raman spectra for direct backscattering along $z \| c$ and $x \perp c$ axes under different polarization conditions. Observed are all phonons allowed in backscattering. The inset shows the low-energy region of the E_2^1 band. Phonon energies are summarized in Table I.

tive relaxed energies, implying tensile stress in the AlN. The E_2^1 exhibits a slight blueshift, as expected from its negative mode-Grüneisen parameter.[45] It is well known that the A_1(LO) phonon will interact with a free-carrier plasma if the plasma is present due to intentional or unintentional doping. The A_1(LO) band loses intensity with increasing carrier concentrations in GaN,[46] and it is reasonable to anticipate the same effect in AlN. Our A_1(LO) to E_2^2 relative intensities for AlN are comparable to what we measure for GaN with low free-carrier concentration ($<10^{17}\,\mathrm{cm}^{-3}$).[47] In our best samples the E_2^2 mode has a narrow FWHM of 6.2 cm^{-1}, which is comparable to 5.6 and 7.2 cm^{-1} reported for AlN grown on sapphire and SiC substrates, respectively.[48] The presence of all phonon modes allowed in backscattering measurements and their narrow linewidths confirm the high crystalline quality of the wurtzite AlN studied here.

We now describe our determination of the Raman-stress factor. All measurements were carried out on samples with 0.2-μm thickness. Noting the tendency of decreasing stress with increasing thickness,[49] we chose samples with minimum thicknesses that can be measured with an acceptable signal-to-noise ratio by both Raman and XRD techniques. The greater stress will give us larger differences in the Raman energy and lattice parameter, affording the best possible precision in determining the Raman-stress factor.

To determine the zero-stress value of the E_2^2 phonon energy, we back-thinned the silicon substrate from a 0.8-μm-thick AlN film using standard chemical etching. A free-standing crystal approximately $50\,\mu\mathrm{m} \times 50\,\mu\mathrm{m}$ square was cleaved for micro-Raman measurements. Although there may be some residual stress, we expect this to be small in comparison to that caused by a substrate. For this free-standing crystal we found the E_2^2 band energy of $657.4 \pm 0.2\,\mathrm{cm}^{-1}$, which is the same value obtained in Ref. 35 for a relaxed (7-μm-thick) AlN film grown on sapphire. An undoped AlN film grown on sapphire will be either relaxed or under biaxial compressive stress. Conversely, an undoped AlN film grown on silicon will be either relaxed or under biaxial tensile stress. The fact that both films reveal the same E_2^2 phonon position argues that the $657.4 \pm 0.2\,\mathrm{cm}^{-1}$ value accurately reflects the zero-stress energy.

TABLE II. Literature values of the relevant elastic stiffness tensor elements. The last column is the Raman-stress factor for the E_2^2 phonon of AlN calculated using our data and the listed elastic constants.

Reference	C_{11} (GPa)	C_{12} (GPa)	C_{13} (GPa)	C_{33} (GPa)	k (cm^{-1}/GPa)
35	419	177	140	392	-6.3 ± 1.4
33	345	125	120	395	-6.7 ± 1.5
34	411 ± 10	149 ± 10	99 ± 3.5	398 ± 10	-4.4 ± 1.0
36	410	140	100	390	-4.5 ± 1.0
39	396	137	108	373	-5.4 ± 1.3

XRD determination of the change in the conventional cell length along the c axis gives a strain $e_\| = \Delta c/c_0$ of $-(2.16 \pm 0.26) \times 10^{-3}$. These measurements were from five samples all with a thickness of about 0.2 μm and each exhibiting the same E_2^2 phonon energy shift of $-9.5 \pm 0.2\,\mathrm{cm}^{-1}$, within experimental error. Multiple (mapping) measurements revealed good uniformity in the stress across the wafer. We use $c_0 = 0.4980\,\mathrm{nm}$.[50] The biaxial stress is determined using

$$\sigma_\perp = \left[(C_{11} + C_{12}) - \frac{2C_{13}^2}{C_{33}} \right] e_\perp , \tag{4}$$

where $e_\perp$ is the strain in the growth plane, which is proportional to the strain along the c axis ($e_\|$)

$$e_\| = -\frac{2C_{13}}{C_{33}} e_\perp . \tag{5}$$

C_{ij} are the elastic constants of AlN. We report here the Raman stress factor of $k = -6.3 \pm 1.4\,\mathrm{cm}^{-1}$/GPa for the E_2^2 phonon of AlN calculated using our combined Raman and XRD measurements and the recent elastic constants of Davydov *et al.*, which were based on epitaxial AlN.[35] For completeness, we include in Table II the values of k calculated using other sets of elastic constants. Variation in k is evident in Table II originating from the different sets of C_{ij}. Nevertheless, all the calculated Raman factors are within total error of each other.

Since we find no reports of Raman stress factors for AlN in the literature, we compare our value with what has been reported for wurtzite GaN. A brief survey of articles gives a range of values: -2.7 (Ref. 20), -4.1 (Ref. 26), -6.2 (Ref. 49), and -7.7 cm^{-1}/GPa (Ref. 51) from biaxially stressed GaN on sapphire. Our measurement for AlN is within the

range of reported values for GaN. Although we do not know the reasons for the large spread in Raman-stress factors of GaN, we would like to emphasize that the study of highly uniform epilayers is essential for an accurate determination. This is because Raman scattering measurements probe a relatively small excitation area (of the order of μm^2 to 0.1 mm^2), providing local information on any film in which there may be spatial variation in the stress. In contrast, XRD probes a much larger area (of the order of mm^2), providing an average strain property.

Using the shifts measured in the E_2^2 phonon energy and our Raman-stress factor, we can calculate stress in AlN using Eq. (1). We measured the stress in films having different thicknesses (0.2–0.8 μm). We find that the stress generally decreases with increasing AlN thickness. The maximum stress we observe is 1.5 ± 0.4 GPa in our 0.2-μm-thick samples. Since the thermal expansion coefficient of AlN is larger than that of Si, the epitaxial layer is subjected to biaxial tensile stress when the sample cools following growth. Using the thermal expansion coefficients of silicon (Ref. 52) and AlN (Ref. 53) we expect a biaxial tensile stress in AlN of $\approx$0.7 GPa. The additional 0.8-GPa stress present in our 0.2-μm AlN layers is attributed to the residual stress present due to incomplete relaxation of the AlN layer at the growth temperature. In the 0.8-μm-thick sample, for which the Raman data are shown in Fig. 4 and summarized in Table I, we use the E_2^2 phonon energy (653.6 cm^{-1}) to obtain the tensile stress of 0.6 ± 0.2 GPa. This is consistent with our estimation for the stress due to the thermal expansion mismatch of AlN and Si.

V. SUMMARY AND DISCUSSION

The FTIR reflectance spectra show a drastic variation in character (Fig. 2) over the 0.06–0.80-μm range of thicknesses studied. These spectra are well described by a model using damped Lorentzian oscillators for the dielectric functions, taking into account the anisotropy of the AlN wurtzite structure. The A_1- and E_1-symmetry phonon energies and the AlN layer thicknesses are the primary parameters in the model.

Raman spectra show all phonons allowed in a direct backscattering configuration (Fig. 4). Phonon energies agree with the FTIR measurements and with previous studies (primarily Raman scattering of AlN grown on sapphire). The E_2^2 phonon energy for AlN under no stress is found to be 657.4 $\pm 0.2\ cm^{-1}$. By using combined Raman and XRD measurements, we obtain a Raman-stress factor for biaxial stress on AlN of $-6.3 \pm 1.4\ cm^{-1}$/GPa. As is evident in Table II, the Raman-stress factor based on our measurements is strongly affected by the values for the elastic constants. These vary substantially between reports. The same conclusion was reached by Kisielowski *et al.*[26] in connection with GaN. Further measurements, aimed at finding an accepted set of elastic constants, are needed to improve our understanding of the effects of stress, in general. Stress in AlN due to the silicon substrate is tensile, inducing a redshift to the E_2^2 band. The stresses ranged between 0.6 and 1.5 GPa. The thermal expansion mismatch between AlN and the silicon substrate results in a stress of approximately 0.6 GPa. The additional stress seen in some layers is attributed to residual stress, which occurs during growth.

The stresses measured in AlN are quite large. In our previous work concerning GaN grown on silicon, we measured a biaxial tensile stress of 0.40 GPa.[23] This stress was well described by the thermal expansion mismatch between the epilayer and the silicon. GaN grown on sapphire is subjected to large biaxial compressive stresses, ranging from 0.4 to 1 GPa.[26] A stress value of 1.3 GPa has been observed recently in $Al_xGa_{1-x}N$ layers grown on sapphire.[54] This is very close in magnitude to the largest stress we have seen in our AlN/Si samples. Even larger stresses (6.3 GPa) have been reported in GaN-AlN superlattices grown on sapphire.[55] Evidently, large stresses are typical in the nitride system of semiconductors when they are epitaxially deposited on common substrates. The ability for the nitride layers to withstand such stresses depends on the uniformity, crystal quality, and layer thickness.

ACKNOWLEDGMENTS

The authors wish to acknowledge Professor V. Levitas for useful discussions and A. Konkar for the AFM measurements. M.H. acknowledges partial support from the State of Texas Advanced Technology Program. The work at Texas Tech University was supported by the AFOSR (F49620-97-1-0289), DARPA (F19628-99-C-0013) and the National Science Foundation (ECS-0070240). J.V. acknowledges support from the National Science Foundation (DMR-9705498).

*Email address: Mark.Holtz@ttu.edu

[1] S. C. Jain, M. Willander, J. Narayan, and R. Van Overstraeten, J. Appl. Phys. **87**, 965 (2000).

[2] T. Shiosaki, T. Yamamoto, T. Oda, and A. Kawabata, J. Appl. Phys. **36**, 643 (1980).

[3] Y. F. Wu, B. P. Keller, J. Fina, J. Pusl, M. Le, N. X. Nguyen, C. Nguyen, D. Widman, S. Keller, S. P. Denbaars, and U. K. Mishra, Electron. Lett. **33**, 1742 (1977).

[4] J. Meinschien, F. Falk, H. Hobert, and H. Stafast, Appl. Surf. Sci. **138-139**, 543 (1999).

[5] A. Ohtani, K. S. Stevens, and R. Beresford, Appl. Phys. Lett. **65**, 61 (1994).

[6] E. Callerja, M. A. Sánchez-García, E. Monroy, F. J. Sánchez, E. Muñoz, A. Sanz-Hervás, C. Villar, and M. Aguilar, J. Appl. Phys. **82**, 4681 (1997).

[7] K. Yasutake, A. Takeuchi, H. Kakiuchi, and K. Yoshii, J. Vac. Sci. Technol. A **16**, 2140 (1998).

[8] A. Bourret, A. Barski, J. L. Rouviere, G. Renaud, and A. Barbier, J. Appl. Phys. **83**, 2003 (1998).

[9] S. A. Nikishin, V. G. Antipov, S. Francoeur, N. N. Faleev, G. A. Seryogin, V. A. Elyukhin, H. Temkin, T. I. Prokofyeva, M. Holtz, A. Konkar, and S. Zollner, Appl. Phys. Lett. **75**, 484 (1999).

[10] S. A. Nikishin, N. N. Faleev, H. Temkin, and S. N. G. Chu,

Electrochem. Soc. Proc. **99-17**, 238 (1999).
[11] S. A. Nikishin, N. N. Faleev, V. G. Antipov, S. Francoeur, L. Grave de Peralta, G. A. Seryogin, T. I. Prokofyeva, M. Holtz, S. N. G. Chu, A. S. Zubrilov, Y. Melnik, V. Dmitriev, and H. Temkin, MRS Internet J. Nitride Semicond. Res. **5S1**, W8.3 (2000).
[12] G. D. Kipshidze, H. P. Shenk, A. Fissel, U. Kaiser, J. Schulze, Wo. Richter, M. Weinacht, R. Kunze, and J. Kräusslich, Semiconductors **33**, 1241 (1999).
[13] A. T. Collins, E. C. Lightowlers, and P. J. Dean, Phys. Rev. **158**, 833 (1967).
[14] I. Akasaki and M. Hashimoto, Solid State Commun. **5**, 851 (1967).
[15] M. F. MacMillan, R. P. Devaty, and W. J. Choyke, Appl. Phys. Lett. **62**, 750 (1993).
[16] H. P. Schenk, U. Kaiser, G. D. Kipshidze, A. Fissel, J. Kräußlich, H. Hobert, J. Schulze, and Wo. Richter, Mater. Sci. Eng. B **59**, 84 (1999).
[17] K. S. Jagannadham, S. K. Sharma, Q. Wei, R. Kalyanraman, and J. Narayan, J. Vac. Sci. Technol. A **16**, 2804 (1998).
[18] R. Y. Krupitskaya and G. W. Auner, J. Appl. Phys. **84**, 2861 (1998).
[19] R. D. Vispute, J. Narayan, and J. D. Budai, Thin Solid Films **299**, 94 (1997).
[20] V. Yu. Davydov, N. S. Averkiev, I. N. Goncharuk, D. K. Nelson, I. P. Nikitina, A. S. Polkovnikov, A. N. Smirnov, M. A. Jacobson, and O. K. Semchinova, J. Appl. Phys. **82**, 5097 (1997).
[21] T. E. Tiwald, J. A. Woolam, S. Zollner, J. Christiansen, R. B. Gregory, T. Wetteroth, S. R. Wilson, and A. R. Powell, Phys. Rev. B **60**, 11 464 (1999).
[22] D. W. Berreman, Phys. Rev. **130**, 2193 (1963).
[23] M. Seon, T. Prokofyeva, M. Holtz, S. A. Nikishin, N. N. Faleev, and H. Temkin, Appl. Phys. Lett. **76**, 1842 (2000).
[24] B. Monemar, J. P. Bergman, and I. A. Buyanova, in *GaN and Related Materials*, edited by S. J. Pearton (Gordon and Breach, New York, 1997).
[25] B. Gil, in *Gallium Nitride II*, edited by J. I. Pankove and T. D. Moustakas (Academic, Boston, 1999), Vol. 57.
[26] C. Kisielowski, J. Krüger, S. Ruvimov, T. Suski, J. W. Ager, E. Jones, Z. Liliental-Weber, M. Rubin, E. R. Weber, M. D. Bremser, and R. F. Davis, Phys. Rev. B **54**, 17 745 (1996).
[27] H. Siegle, P. Thurian, L. Eckey, A. Hoffmann, C. Thomsen, B. K. Meyer, H. Amano, I. Akasaki, T. Detchprohm, and K. Hiramatsu, Appl. Phys. Lett. **68**, 1265 (1996).
[28] M. Holtz, M. Seon, T. Prokofyeva, H. Temkin, R. Singh, F. P. Dabkowski, and T. D. Moustakas, Appl. Phys. Lett. **75**, 1757 (1999).
[29] C. Balkas, Z. Sitar, T. Zheleva, L. Bergman, R. Nemanich, and R. F. Davis, J. Cryst. Growth **179**, 363 (1997).
[30] L. Bergman, M. Dutta, C. Balkas, R. F. Davis, J. A. Christman, D. Alexson, and R. J. Nemanich, J. Appl. Phys. **85**, 3535 (1999).
[31] O. Brafman, G. Lengyel, S. S. Mitra, P. J. Gielisse, J. N. Plendl, and L. C. Mansur, Solid State Commun. **6**, 523 (1968).
[32] E. Anastassakis, A. Pinczuk, E. Burstein, F. H. Pollak, and M. Cardona, Solid State Commun. **8**, 133 (1970).
[33] K. Tsubouchi, K. Sugai, and N. Mikoshiba, in *Ultrasonics Symposia Proceedings*, edited by B. R. McAvoy (IEEE, New York, 1981), p. 375.
[34] L. E. McNeil, M. Grimsditch, and R. H. French, J. Am. Ceram. Soc. **76**, 1132 (1993).
[35] V. Yu. Davydov, Yu. E. Kitaev, I. N. Goncharuk, A. N. Smirnov, J. Graul, O. Semchinova, D. Uffmann, M. B. Smirnov, A. P. Mirgorodsky, and R. A. Evarestov, Phys. Rev. B **58**, 12 899 (1998).
[36] C. Deger, E. Born, H. Angerer, M. Stutzmann, J. Hornsteiner, E. Riha, and G. Fischerauer, Appl. Phys. Lett. **72**, 2400 (1998).
[37] E. Ruiz, S. Alvarez, and P. Alemany, Phys. Rev. B **49**, 7115 (1994).
[38] K. Kim, W. R. L. Lambrecht, and B. Segall, Phys. Rev. B **53**, 16 310 (1996).
[39] A. F. Wright, J. Appl. Phys. **82**, 2833 (1997).
[40] S. A. Nikishin (unpublished).
[41] T. E. Tiwald, D. W. Thompson, J. A. Woolam, W. Paulson, and R. Hance, Thin Solid Films **313-314**, 661 (1998).
[42] R. M. A. Azzam and N. M. Bashara, *Ellipsometry and Polarized Light* (North-Holland, New York, 1977).
[43] M. Schubert, M. A. Kasic, T. E. Tiwald, J. Off, B. Kuhn, and F. Scholz, MRS Internet J. Nitride Semicond. Res. **4**, 1 (1999).
[44] W. G. Spitzer in *Optical Properties of III-V Compounds*, Vol. 3 of Semiconductors and Semimetals, edited by Willardson and A. C. Beer (Academic, New York, 1967), p. 17.
[45] K. Karch, J.-M. Wagner, H. Siegle, C. Thomsen, and F. Bechstedt, Mater. Sci. Forum **264-268**, 303 (1998).
[46] P. Perlin, J. Camassel, W. Knap, T. Taliercio, J. C. Chervin, T. Suski, I. Grzegory, and S. Porowski, Appl. Phys. Lett. **67**, 2524 (1995).
[47] T. Prokofyeva (unpublished).
[48] K. Kornitzer, W. Limmer, K. Thonke, R. Sauer, D. G. Ebling, L. Steinke, and K. W. Benz, J. Cryst. Growth **201-202**, 441 (1999).
[49] T. Kozawa, T. Kachi, H. Kano, Y. Taga, M. Hashimoto, N. Koide, and K. Manabe, J. Appl. Phys. **75**, 1098 (1994).
[50] H. Schultz and K. H. Thiemann, Solid State Commun. **23**, 815 (1977).
[51] I. H. Lee, I. H. Choi, C. R. Lee, E. J. Shin, D. Kim, S. K. Noh, S. J. Son, K. Y. Lim, and H. J. Lee, J. Appl. Phys. **83**, 5787 (1998).
[52] Y. Okada and Y. Tokumaru, J. Appl. Phys. **56**, 314 (1984).
[53] K. Wang and R. R. Reeber, in *Nitride Semiconductors*, Mater. Res. Soc. Symp. Proc. No. 482, edited by F. A. Ponce, S. P. DenBaars, B. K. Meyer, S. Nakamura, and S. Strite (Materials Research Society, Warrendale, PA, 1998), p. 863.
[54] J. Han, M. N. Crawford, R. J. Shul, S. J. Hearne, E. Chason, J. J. Figiel, and M. Banas, MRS Internet J. Nitride Semicond. Res. **4S1**, G7.7 (1999).
[55] J. Gleize, F. Demangeot, J. Frandon, M. A. Renucci, F. Widmann, and B. Daudin, Appl. Phys. Lett. **74**, 703 (1999).